AUTOMATED 3-D INTRAOCULAR ULTRASOUND DETECTION OF ELEVATED INTRACRANIAL PRESSURE

Yaoqi Zhang[1], W. Clem Karl[1], Gwendolyn Van Der Wilden[2], Peter Fagenholz[2], Javier Romero[3,4], Vicki Noble[2,4], Homer Pien[3,4]

[1]Department of Electrical and Computer Engineering, Boston University, Boston, MA
[2]Department of Emergency Medicine, Massachusetts General Hospital, Boston, MA
[3]Department of Radiology, Massachusetts General Hospital, Boston, MA
[4]Harvard Medical School, Boston, MA

ABSTRACT

Elevated intracranial pressure (ICP) is often associated with traumatic brain injury and can cause substantial complications. Elevated ICP also causes dilation of the optic nerve sheath, which can be observed and quantitated using intraocular ultrasound. We report on the use of 3-D ultrasound and automated processing algorithms to reduce operator variability in the assessment of sheath diameter. Using data from three subjects, we show that our approach appears to reduce operator variability by approximately 25%. These encouraging preliminary results support the development of an intraocular ultrasound system for non-invasive detection of elevated ICP.

Index Terms— ultrasound, anisotropic diffusion, traumatic brain injury (TBI), optic nerve sheath diameter (ONSD), intracranial pressure (ICP).

1. INTRODUCTION

Traumatic brain injuries (TBI) is a major cause of morbidity and mortality in the U.S., with approximately 1.4 million incidents reported annually [1]. Elevated intracranial pressure (ICP) is commonly associated with TBI and other neuro-critical injuries and diseases, and prompt intervention of such patients is vital to their outcome [2,3]. This is due to the recognition that only part of the damage to the brain in TBI occurs at the moment of impact; subsequent secondary insults can include cerebral edema, hemorrhage, hydrocephalus, and ischemia [4]. The current gold standard for monitoring ICP involves the deployment of devices inside the brain - intraventricular and intraparenchymal monitors. These devices are resource intensive and suffer from small but nonetheless significant risk of infection and hemorrhage [4,5]. The development and validation of non-invasive techniques which can be used at bed-side, near the place of injury (e.g., battlefield, scene of car accidents), or during transit to the hospital is therefore invaluable. In this paper we describe an automated approach to using intraocular ultrasound to non-invasively assess ICP.



Figure 1. Intraocular ONSD image. Shown is a single slice of a 3-D acquisition, with anatomic and measurement features labeled.

The optic nerve connects the brain to the eye via a sheathed pathway, terminating at the optic disk of the retina. The sheath is a continuation of the dura layer of the brain, and the subarachnoid space of the brain extends along the optic nerve within the sheath and surrounds the nerve with cerebrospinal fluid [6]. Because of this direct connection, a rise in ICP is transmitted along the sheath and results in a dilation of the optic disk. Although dilation of the optic nerve can be seen using CT or MRI, ultrasound through the lens of the eye represents a highly portable means of non-invasive detection of elevated ICP [7,8].

The use of handheld ultrasound probes to image the optic disk through the eye lid and the lens is well established. These studies typically segregate the patient population into those with normal ICP from those with intracranial hypertension (ICP > 20 cm H_2O). The ultrasound operator images the optic nerve sheath diameter (ONSD), and the feature correlated with ICP is the diameter of the sheath 3 mm back from the optic disk (Figure 1) [9]. Two meta-analyses have shown that, using a sheath diameter of 5 mm as the predictor of intracranial

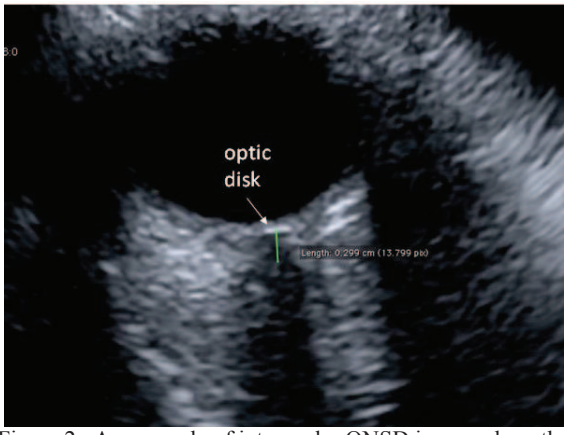


Figure 2. An example of intraocular ONSD image where the boundaries of the sheath 3 mm below the optic disk, at the end of the green caliper segment, are difficult to delineate precisely.

hypertension, pooled detection sensitivity of 90% and 87%, respectively, and specificity of 87% and 80%, respectively, is achieved [10,11].

One issue with intraocular ultrasound ONSD measurements is that of the measurement variance [11,12]. We believe this variability arises in two ways. First, with standard 2-D ultrasound probe, the operator sweeps the probe across the globe of the eye to locate the optic disk, and as such the sweeping motion, rate of sweep, and aspect angle all contribute to the variability. Second, as shown in Figure 2, the resulting ultrasound image can be highly noisy, and as such the quantitation of the sheath diameter is also highly operator dependent. In this paper we attempt to remedy both of these issues. We hypothesize that, by using a 3-D ultrasound probe and eliminating the sweeping motion, variability is reduced. We further hypothesize that the use of an automated segmentation algorithm which estimates the location of the optic nerve sheath from all available 3-D data reduces the sheath diameter quantitation error.

This paper is organized as follows. In Section 2 we describe our processing formulation. In Section 3 our experimental methods are described. Results are described in Section 4, and we discuss the implications of our findings in Section 5.

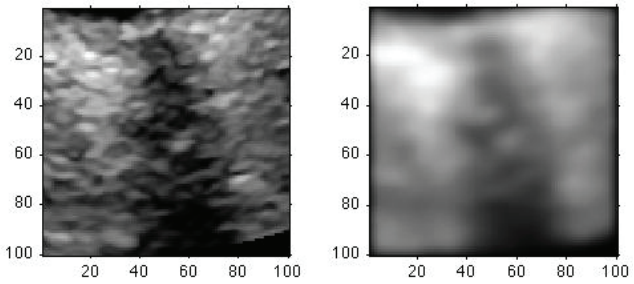


Figure 3. Using anisotropic diffusion to reduce the impact of ultrasound speckle noise. Shown are (L) original ultrasound image, and (R) smoothed image.

2. IMAGE PROCESSING FORMULATION

A number of processing steps is used to determine the ONSD. Since the focus of this paper is on the image processing and parameter estimation, we only briefly mention that the first steps in our processing are to use Chan-Vese [13] in 3-D to create a segmented image from which we fit a sphere to the data in order to identify the globe of the eye. We then localize a region of interest (100 x 100 x 50 pixels) containing the optic nerve sheath on the far side of the globe. All subsequent processing takes place within this region of interest.

To characterize ONSD, two major steps are taken. First, we de-noise the image by using anisotropic diffusion. Second, we identify relevant edge points and fit a parabola to these points in order to characterize the sheath; we assume the sheath is characterized by a 3-D parabola with an elliptical cross section.

2.1 Anisotropic Diffusion

Let *I(x,y,z)* denote the acquired 3-D ultrasound image, and I_t the anisotropic diffusion smoothed image parameterized by the diffusion time *t* [14]:

$$I_t = \mathrm{div}(c \cdot \nabla I) = c \cdot \Delta I + \nabla c \cdot \nabla I$$

where div denotes the divergence, ∇ the gradient, and Δ the Laplacian,

$$c = \exp\left(-\left[-\frac{\|\nabla I\|}{K}\right]^2\right)$$

and *K* is a parameter which controls sensitivity to the presence of edges. The result of applying anisotropic diffusion to reduce the effect of speckle noise is shown in Figure 3.

2.2 Sheath Parameter Estimation

The boundaries of the sheath are assumed to follow a 3-D parabola. The parabola with vertex at (x_c, y_c, z_c) and an elliptical cross section is given by the set of points which satisfies

$$\Omega = \{(x,y,z) \mid \alpha(x - x_c) - [\beta(y - y_c)]^2 - (z - z_c)^2 = 0\}$$

Since the parabola is in general tilted, the above equation needs to be further parameterized by the rotation matrix

$$\omega = \begin{bmatrix} \sin\theta\cos\varphi & -\sin\varphi & \cos\theta\cos\varphi \\ \sin\theta\sin\varphi & \cos\varphi & \cos\theta\sin\varphi \\ -\cos\theta & 0 & \sin\theta \end{bmatrix}$$

where θ denotes the elevation angle and φ the azimuth angle in the x,y-plane.

We follow the formulation of Chan-Vese's fitting model to define a cost functional for optimizing the selection of the parabola [13]. Let $\omega\Omega$ denote the tilted parabola. For any boundary *C*, we define the two mutually exclusive regions *inside(C)* and *outside(C)* as the set of

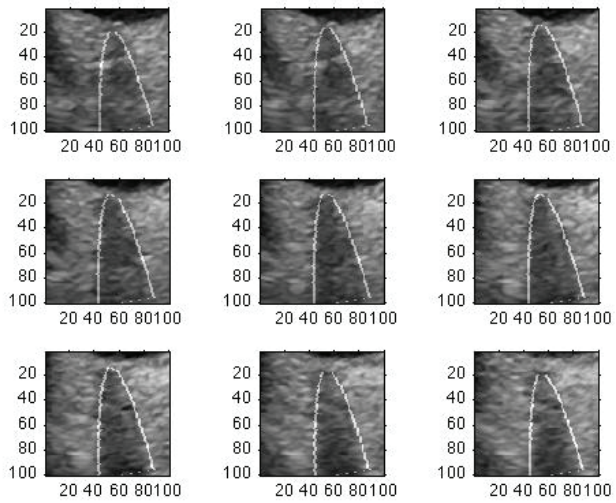


Figure 4. Outline of the estimated parabola for a single subject on 9 consecutive ultrasound images.

points inside and outside, respectively, of the boundary *C*. We now define the cost functional

$$f(\Omega,\omega)=\lambda_1\int_{inside(\omega\Omega)}|I_t(x,y,z)-\mu_{inside}|^2dxdydz$$

$$+\lambda_2\int_{outside(\omega\Omega)}|I_t(x,y,z)-\mu_{outside}|^2dxdydz$$

where μ_{inside} and $\mu_{outside}$ denotes the mean intensity values (of the diffusion smoothed image) of the pixels inside and outside, respectively, of the boundaries of the parabola. That is, we search over the parameters of the basic elliptical parabola $(x_c, y_c, z_c, \alpha, \beta)$ and the rotation matrix (θ, φ) to find the boundaries of a tilted parabola which optimally separates the inside pixels from the outside ones.

3. EXPERIMENTAL METHODS

With IRB approval, subjects who have consented to being in the study were scanned using the Logiq 9 (GE Healthcare) 4-D ultrasound machine. Each subject had a ventriculostomy monitor in place which provided ICP measurements. Each subject was scanned by two different operators.

All data collected on the ultrasound machine were transferred to our institutional PACS system. These ultrasound images were subsequently downloaded to an Apple Mac Pro running 32-bit Osirix. Anonymization to remove patient name, medical record number, and all other identifying information was performed using Osirix.

Ultrasound images were processed using Matlab on Intel-based PC workstations. Each dataset is 532 x 434 pixels in-plane, and the number of slices varied between 126 to 151 from dataset to dataset. The in-plane resolution is 0.178 mm in both x- and y-directions.

4. RESULTS

Using the formulation described in Section 2, ultrasound images for several subjects were processed. Figure 4 shows an example of the processing on a single subject, illustrating the outline of the tilted elliptical parabola on 9 consecutive axial ultrasound slices.

Optic nerve sheath boundaries, modeled as parabolas, were extracted from the 3-D ultrasound images of four eyes from three subjects. For each eye, a number of measurements were taken by two ultrasound operators during the same imaging session. Sometimes an operator would perform a single data acquisition, and at times the data acquisition was repeated. This resulted in either 3 or 4 3-D ultrasound datasets per eye. From the estimated sheath outlines, three parameters were extracted – at 3 mm back from the vertex of the parabola (which ostensibly corresponds to the optic disk), we computed the radius of the short-axis of the elliptical cross section, the radius of the long-axis, and the cross sectional area of the ellipse. These parameters are summarized in Table 1. In particular, Table 1 shows the mean and standard deviation of the measurements, the corresponding standard error (standard deviation / mean), and the number of measurements over which these statistics were obtained.

Table 1. Results summarizing the findings from using automated processing algorithms. Shown are results on four eyes with repeated measurements, for three extracted features: radius of the short axis, long axis, and area at 3-mm from the optic disk.

	eye 1	*eye 2*	*eye 3*	*eye 4*
SHORT AXIS AT 3-MM				
mean	2.28	1.72	2.39	1.97
st dev	0.10	0.10	0.06	0.08
st error	4.5%	5.8%	2.7%	4.0%
num meas	3	4	4	4
LONG AXIS AT 3-MM				
mean	3.70	2.45	3.88	3.20
st dev	0.17	0.14	0.10	0.13
st error	4.5%	5.8%	2.7%	4.0%
num meas	3	4	4	4
AREA AT 3-MM				
mean	26.57	13.27	29.13	19.87
st dev	2.37	1.54	1.55	1.56
st error	8.9%	11.6%	5.3%	7.9%
num meas	3	4	4	4

5. DISCUSSIONS

In this paper we described our initial results from applying image processing and parameter estimation algorithms to the extraction of optic nerve sheath parameters which can

potentially correlate with the presence of intracranial hypertension, using 3-D ultrasound image data. We used anisotropic diffusion as the primary means for reducing the speckle noise in the ultrasound images. We further devised a cost functional, the minimization of which provides the parameters of a tilted 3-D parabola with an elliptical cross section. From these parameters, we computed three features corresponding to the elliptical cross section of the parabola 3 mm from the vertex; these are the radius of the short axis, radius of the long axis, and the cross sectional area of the ellipse. The 3 mm distance was chosen to be consistent with past clinical studies which validated the sheath diameter at 3 mm behind the optic disk as a predictor of intracranial hypertension.

Although there is growing evidence for using ultrasound-based ONSD measurements for elevated ICP, there is also concern over variability associated with using traditional 2-D ultrasound probes and the subsequent subjective measurement of the sheath diameter. Indeed, in one study, it was shown that the standard error on 3 measurements across 20 eyes were 5.61%. In our study, we examined either 3 or 4 measurements across 4 eyes performed by 2 operators for each eye, and obtained an average standard error of 4.25% when examining either the long axis or the short axis radius.

The fact that we were able to demonstrate ~ 25% decrease in the standard error shows that there is promise in our approach of using a combination of 3-D ultrasound and automated image processing algorithms. It should be noted, however, that there wasn't sufficient diversity in the range of ICP's in our sample to allow an assessment of whether the features extracted correlates to the presence of intracranial hypertension. That is, past studies have focused on the in-plane diameter of the sheath 3 mm back from the optic disk. The parameter we have extracted – that of either the long or the short axis radius – may not lie within the plane of the axial image, and as such will require further validation as a predictor of intracranial hypertension.

One issue with our study is that the 3-D ultrasound dataset - although stored in DICOM format - does not record the between-slice (z) resolution. In order to estimate the z-resolution, we make the simplifying assumption that the globe of the eye is a sphere, and the z-resolution is computed as the scale factor which makes the globe as spherical as possible. Although an inaccurate z-resolution value would not alter the primary result of this paper (that of the improvement in parameter variability), it may affect the mean value of the extracted features, and thus the accuracy with which these features may predict intracranial hypertension. We are working with the manufacturer of the ultrasound machine to rectify this problem.

6. REFERENCES

[1] J.J. Bruns, A.S. Jagoda, "Mild traumatic brain injury," *Mt. Sinai J. Medicine*, 2009, 76, 145-62.

[2] N.J. Cowley, E.J. Da Silva, "Prevention of secondary brain injury following head trauma," *Trauma*, 2008.

[3] S.C. Stein, G.S. Young, R.C. Talucci, et al., "Delayed brain injury after head trauma: significance of coagulopathy," *Neurosurgery*, 1992, 30.

[4] A.R. Frattalone, R.D. Stevens, "Intracranial pressure and its surrogates," *Intensive Care Med.*, 2011, 37, 1051-53.

[5] K. Rickert, G. Sinson, "Intracranial pressure monitoring," *Operative Techniques in General Surgery*, 2003, 5, 170-5.

[6] V. Rajajee, M. Vanaman, J. J. Fletcher, T. L. Jacobs, "Optic nerve ultrasound for the detection of raised intracranial pressure," *Neurocritical Care*, 2011, epub.

[7] R.I. Silver, G. Moonis, R.J. Schlosser, et al., "Radiographic signs of elevated intracranial pressure in idiopathic cerebrospinal fluid leaks: a possible presentation of idopathic intracranial hypertension," Am. J. Rhinology, 2007, 21, 257-61.

[8] H.H. Kimberly, V.E. Noble, "Using MRI of the optic nerve sheath to detect elevated intracranial pressure," *Critical Care*, 2008, 12, 181-2.

[9] H.H. Kimberly, S. Shah, K. Marill, V. Noble, "Correlation of optic nerve sheath diameter with direct measurement of intracranial pressure," *Academic Emergency Med.*, 2008, 15, 201-4.

[10] J. Dubourg, E. Javouhey, T. Geeraerts, "Ultrasonography of optic nerve sheath diameter for detection of raised intracranial pressure: a systematic review and meta-analysis," *Intensive Care Med.*, 2011, 37, 1059-68.

[11] R. Moretti, B. Pizzi, "Ultrasonography of the optic nerve in neurocritically ill patients," *Acta. Anesthesiol. Scand.*, 2011, 55, 644-52.

[12] S. Shah, H. Kimberly, K. Marill, V.E. Noble, "Ultrasound techniques to measure the optic nerve sheath: is a specialized probe necessary?" *Med. Sci. Monitor*, 2009, 15, 63-8.

[13] T. F. Chan, L. A. Vese, "Active contours without edges," *IEEE Trans. Image Proc.*, 2001, 10, 266-77.

[14] P. Perona, J. Malik, "Scale-space and edge detection using anisotropic diffusion," *IEEE Patt. Analy. Mach. Intel.*, 1990, 12, 629-39.